$DAN/LANGLEY$
$IN-34$
$69617 -CR$

DEPARTMENT OF MECHANICAL ENGINEERING AND MECHANICS
SCHOOL OF ENGINEERING
OLD DOMINION UNIVERSITY
NORFOLK, VIRGINIA 23508

$P.47$

STABILITY OF STREAMWISE VORTICES

By

M. R. Khorrami, Graduate Research Assistant,

C. E. Grosch, Co-Principal Investigator,

and

R. L. Ash, Principal Investigator

Progress Report
For the period ended April 1, 1986

April 1987

DEPARTMENT OF MECHANICAL ENGINEERING AND MECHANICS
SCHOOL OF ENGINEERING
OLD DOMINION UNIVERSITY
NORFOLK, VIRGINIA 23508

STABILITY OF STREAMWISE VORTICES

By

M. R. Khorrami, Graduate Research Assistant,

C. E. Grosch, Co-Principal Investigator,

and

R. L. Ash, Principal Investigator

Progress Report
For the period ended April 1, 1986

April 1987

STABILITY OF STREAMWISE VORTICES

By

M. R. Khorrami,[1] C. E. Grosch,[2] and R. L. Ash[3]

ABSTRACT

A brief overview of some theoretical and computational studies of the stability of streamwise vortices is given. The local induction model and classical hydrodynamic vortex stability theories are discussed in some detail. The importance of the three-dimensionality of the mean velocity profile to the results of stability calculations is discussed briefly.

In this study the mean velocity profile is provided by employing the similarity solution of Donaldson and Sullivan. The global method of Bridges and Morris was chosen for the spatial stability calculations for the non-linear eigenvalue problem. In order to test the numerical method, a second order accurate central difference scheme was used to obtain the coefficient matrices. It was shown that a second order finite difference method lacks the required accuracy for global eigenvalue calculations. Finally the problem was formulated using spectral methods and a truncated Chebyshev series.

[1] Graduate Research Assistant, Department of Mechanical Engineering and Mechanics, Old Dominion University, Norfolk, Virginia 23508.
[2] Professor, Department of Oceanography and Department of Computer Science, Old Dominion University, Norfolk, Virginia 23508.
[3] Chairman/Eminent Professor, Department of Mechanical Engineering and Mechanics, Old Dominion University, Norfolk, Virginia 23508.

TABLE OF CONTENTS

LIST OF TABLES

TABLE OF CONTENTS

LIST OF TABLES

LIST OF FIGURES

1. INTRODUCTION

The study of the stability of streamwise vortices is an important and challenging problem. The breakdown of leading edge vortices on delta wings, which severely reduces lift, and the very stable wing tip vortices shed from large commercial aircraft, which determine the flight frequency at airports, are two classical examples. Meaningful experimental and computational work is rare due to the complex nature of the phenomena, and theoretical studies are incomplete. The complexity stems from the three-dimensional nature of the problem and hence the necessity of finding three-dimensional mean velocity profiles which are solutions of the Navier-Stokes equations. Most of the stability calculations to date have used Lamb's vortex [Lamb, 1945], and in some cases a Long's vortex [Long, 1958] or solid body rotation superimposed on Poiseuille flow in a pipe as the basic unperturbed flow. Here we give a brief overview of some of the more important theoretical and computational studies of these flows. This review is by no means exhaustive, but the cited papers are those which we have judged most relevant to the present research.

The theory of vortex stability or vortex deformation has progressed in two distinct directions. In the first case one uses a localized-induction model for an inviscid incompressible vortex [Hama, 1962]. The second approach uses the classical hydrodynamic stability theory for rotating fluids and can be attributed to a paper of Howard and Gupta [1962] which contains a generalization of a stability criteria put forward by Lord Rayleigh [1916]. In this summary, we will discuss the development of both theories starting with the localized-induction model.

The deformation of a curved vortex filament under its own influence was first calculated by Hama [1962] using a localized-induction model with the assumptions that the local radius of curvature is much greater than the

core radius and that the vortex filament is unaffected by the events at infinity. He used several initial two-dimensional shapes and found that in every case the region near the vertex of the curve would lift off of the plane of the initial curve causing a three-dimensional helical deformation to take place. The helical wave, which rotates opposite to the circulatory motion of the vortex filament propagates away from the vertex and its amplitude increases as the vortex lifts.

Betchov [1965] extended Hama's work and derived two equations describing the curvature and torsional effect of the vortex filament. After linearizing the equations, he found that the vortex became unstable if the perturbation wavelength was $> 2\pi R$, with R the local radius of curvature. This type of perturbation is generally referred to as a long wavelength instability.

The work of Betchov was extended by Widnall [1972] who considered the effect of sinusoidal disturbances on a helical vortex filament of finite core radius and infinite extent. She found that the helical vortex filament had three distinct modes of instability: a very short wave instability mode where the local radius of curvature of the helix was the characteristic length; a low wave number mode which was found to be due to the local-induction (this instability is the same mode that was identified by Betchov); and the mutual inductance mode. The latter mode sets in whenever the successive turns of the helix get very close to each other. Finally, Widnall found that increasing the vortex core size: (1) reduced the amplification rate of the large wave instability; (2) increased the amplification rate of the mutual-inductance instability; and (3) decreased the wave number of the short-wave mode.

The hydrodynamic stability of a vortex was first studied by Lord Rayleigh [1916]. In his classical paper he was able to show that a necessary and sufficient condition for stability of an inviscid vortex without axial velocity was that the square of circulation must increase outwards. Much later, Howard and Gupta [1962] were able to give a sufficient condition for the stability of an inviscid vortex with axial velocity (subject to axisymmetric disturbances). They found that for stability the local value

$$J(r) \equiv \frac{1}{r^3} \frac{d\Gamma^2}{dr} \Bigg/ (\frac{dW}{dr})^2 > \frac{1}{4}$$

everywhere. Here Γ is the circulation and W is the axial velocity.

It is obvious from the above criterion that axial shear has a destabilizing effect. For non-axisymmetric disturbances, Howard and Gupta found that a sufficient condition for stability was

$$\alpha^2 \phi - \frac{2\alpha n}{r^2} V \frac{dW}{dr} - \frac{1}{4} [\alpha \frac{dW}{dr} + n \frac{d(V/r)}{dr}]^2 > 0$$

where

$$\phi \equiv \frac{1}{r^3} \frac{d(r^2 V^2)}{dr}$$

and V is the tangential velocity, and α and n are the axial and azimuthal wave numbers, respectively. They stated that the above criterion is always violated for sufficiently small α, and while this does not imply instability, it has led them to suggest that no general necessary and sufficient criterion is obtainable.

Using the equation for the radial amplitude of disturbances derived by Howard and Gupta, Pedley [1968] has shown that for a very small Rossby

number ($\varepsilon \equiv \dfrac{W_0}{2\Omega r_0}$, where Ω is the angular velocity) the flow is unstable to non-axisymmetric inviscid disturbances of sufficiently large axial wave-length. He found that, although both solid body rotation and Poiseuille flow in a pipe are stable with respect to infinitesimal disturbances, the superimposed combined flow (which is a helical vortex) is highly unstable with the negative azimuthal wavenumbers as the dominant unstable modes. These disturbances are helical in shape, wrap around the helical vortex in the opposite direction and are either standing waves or are traveling up-stream. The growth rate of the most rapidly growing disturbance is $2\varepsilon\Omega$, where ε is the Rossby number and Ω is the angular velocity of the pipe wall. In a follow-up paper, Pedley [1969] has shown that for viscous, rotating Poiseuille flow the critical Reynolds number, Re_c, has a value of 82.9 corresponding to n = 1. The critical Reynolds number increases as the value of azimuthal wave number, n, increases. The disturbances are stationary relative to the rotating frame of reference, and as the Reynolds number increases, the wave number of the most rapidly growing disturbance also increases.

Maslowe [1974] has studied the same flow field as that of Pedley [1968] without making an assumption as to the magnitude of the Rossby number. He has shown that the most unstable modes have negative azimuthal wave numbers. They spiral in the same direction as the basic flow rotation (note this is in contradiction to Pedley's finding and is caused by different interpreta-tions of what direction a wave with negative azimuthal wave number spirals) but propagate upstream in the axial direction with an axial phase speed $O(\varepsilon^{-1})$. Also, the amplification factor and the axial wave number of the fastest growing disturbance peaked at a finite Rossby number ε of O(1) while the growth rate showed little variation with n for $|n| > 2$ at finite values of ε.

The stability of the mean velocity profile of a trailing line vortex (Batchelor [1964]) was studied by Lessen, Singh, and Paillet [1974] in a study of the inviscid stability of swirling flows with respect to infinitesimal non-axisymmetric disturbances. It was found that negative azimuthal wave numbers are destabilized by the addition of swirl. Lessen, et al. discovered that the stability of the vortex is very dependent on the value of q, where q is given by $\frac{\Gamma_0}{U_s r_s}$, with U_s and r_s the scaling factors for the velocity and radial coordinate, respectively and Γ_0 the constant circulation at large radial distance r_0. All wavelengths appear to become damped, and the flow completely stabilized at a value of q slightly greater than 1.5. Using a finite-difference method, Duck and Foster [1980] have solved exactly the same problem as that of Lessen et al. [1974] and obtained similar results. However, they found that the number of unstable modes is directly dependent on the number of grid points, N, so that as N increases the number of unstable modes increases as well. One has to be skeptical about this finding since the number of unstable modes should not depend on the grid and grow without bound.

Following their earlier work, Lessen and Paillet [1974] performed a viscous stability calculation for a trailing line vortex. They obtained similar results to those of Pedley [1969] which indicated that the critical Reynolds number increases as $|n|$ increases. Their calculations of neutral stability curves showed that the values of the critical wavelength and critical Reynolds number are not very sensitive to the exact value of q; and at large q all of the unstable modes are stabilized for any wavelength and Reynolds number.

Although these calculations are valuable, they do not constitute a systematic study of the effects of different boundary conditions and mean velocity profiles on the stability of the vortex. The need for such a systematic study is the rationale behind the present research. In this study the effect of such parameters as mean velocity profile, vortex Reynolds number $\frac{\Gamma}{\nu}$, and axial pressure gradient $\frac{dP}{dz}$ on vortex stability will be considered. We are going to examine the spatial stability of a rather general class of laminar incompressible vortices in the context of linear theory.

2. MATHEMATICAL FORMULATION OF THE STABILITY PROBLEM

2.1 Mean Velocity Profile

The similarity solution for porous pipe flow due to Donaldson and Sullivan [1960] has been selected as the mean velocity profile. Although one might argue that this similarity solution is for confined flow and its relation to the unconfined flow of longitudinal vortices is not an obvious one, the wealth of different solutions possible (ranging from a single cell vortex to multiple cell vortices) make the selection a reasonable choice. This multiplicity in the core of some vortices has been shown experimentally, (Adams and Gilmore [1972]). These experiments also indicate that in order for a vortex to become unstable, large gradients in the axial direction must develop (Graham and Newman [1974], Leuchter and Solignac [1983]). They have shown that the transition of the axial velocity profile from a strong jet to a strong wake plays a dominant role in the loss of stability of these vortices. Therefore any velocity profile selected for study should show similar behavior.

The mean velocity profiles which we have selected for study are of the form

$$U = U(r)$$
$$V = V(r)$$
$$W = z\overline{W}(r)$$

where, U, V, and W are radial, tangential, and axial velocities, respectively, and r is the distance in the radial direction. Note that the flow undergoes linear acceleration in the streamwise direction. This interesting feature, we believe, may strongly effect the spatial stability of vortices.

Figures 1 thru 3 show three sample mean velocity profiles obtained using Donaldson and Sullivan's similarity solution. The similarity of the tangential velocity in Figs. 1c and 2c to that of Lamb's vortex is noteworthy. Figures 2b and 3b represent the mean velocity profiles of two multiple cell vortices with jet like and wake like axial velocity, respectively. It is important to note that the transition of a vortex core from a jet flow to a wake type can be simulated step by step by changing a few parameters in the similarity solution.

2.2 Perturbations of the Governing Equations

Cylindrical coordinates (r, θ, z) have been chosen as the coordinate system. The equations of motion in cylindrical coordinates are:

continuity

$$\frac{1}{r} \frac{\partial}{\partial r}(ru') + \frac{1}{r}\frac{\partial v'}{\partial \theta} + \frac{\partial w'}{\partial z} = 0 \tag{1}$$

r-momentum

$$\frac{\partial u'}{\partial t} + u'\frac{\partial u'}{\partial r} + \frac{v'}{r}\frac{\partial u'}{\partial \theta} + w'\frac{\partial u'}{\partial z} - \frac{v'^2}{r} =$$

Fig. 1. a) Radial velocity vs. radial distance, b) Axial velocity vs. radial distance, and c) Tangential velocity vs. radial distance.
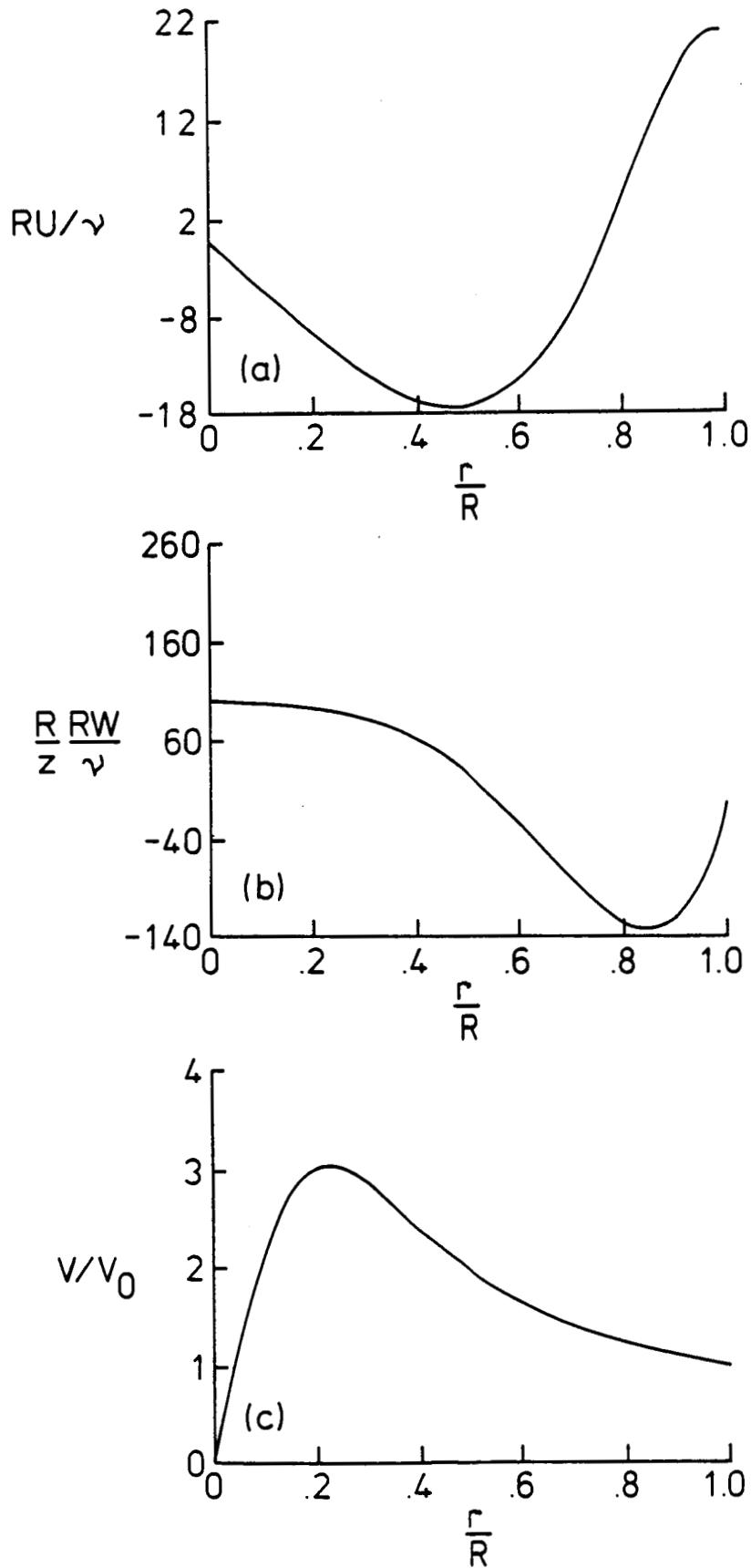
Fig. 2. a) Radial velocity vs. radial distance, b) Axial velocity vs.
radial distance, and c) Tangential velocity vs. radial distance.
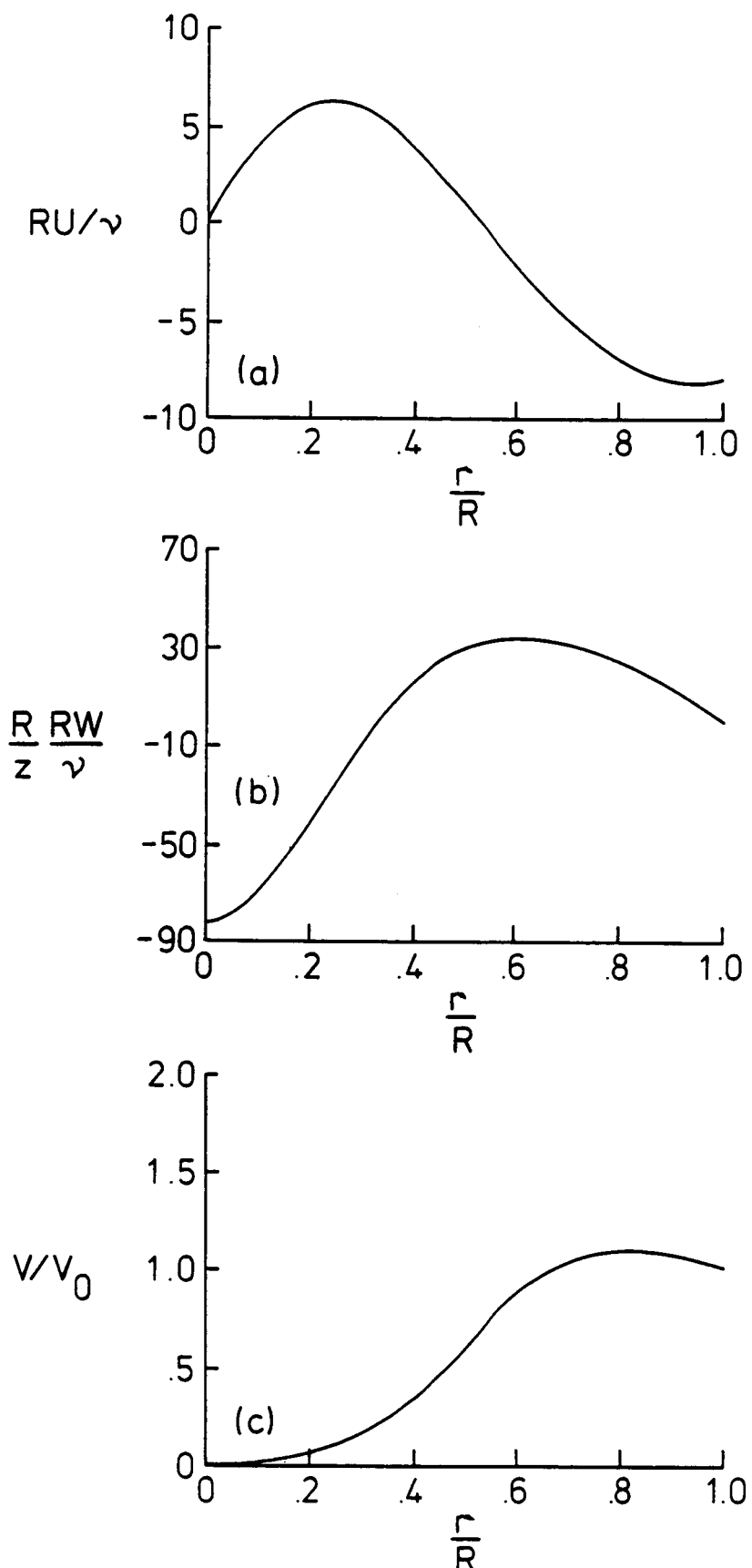
Fig. 3. a) Radial velocity vs. radial distance, b) Axial velocity vs.
radial distance, and c) tangential velocity vs. radial distance.

$$= -\frac{1}{\rho}\frac{\partial p'}{\partial r} + \nu\left(\nabla^2 u' - \frac{u'}{r^2} - \frac{2}{r^2}\frac{\partial v'}{\partial \theta}\right) \tag{2}$$

θ-momentum

$$\frac{\partial v'}{\partial t} + u'\frac{\partial v'}{\partial r} + \frac{v'}{r}\frac{\partial v'}{\partial \theta} + w'\frac{\partial v'}{\partial z} + \frac{u'v'}{r}$$

$$= -\frac{1}{\rho r}\frac{\partial p'}{\partial \theta} + \nu\left(\nabla^2 v' - \frac{v'}{r^2} + \frac{2}{r^2}\frac{\partial u'}{\partial \theta}\right) \tag{3}$$

z-momentum

$$\frac{\partial w'}{\partial t} + u'\frac{\partial w'}{\partial r} + \frac{v'}{r}\frac{\partial w'}{\partial \theta} + w'\frac{\partial w'}{\partial z} = -\frac{1}{\rho}\frac{\partial p'}{\partial z} + \nu\nabla^2 w' \tag{4}$$

where

$$\nabla^2 \equiv \frac{\partial^2}{\partial r^2} + \frac{1}{r}\frac{\partial}{\partial r} + \frac{1}{r^2}\frac{\partial^2}{\partial \theta^2} + \frac{\partial^2}{\partial z^2} \quad .$$

The perturbed flow variables in these coordinates are assumed to be of the form:

$$u' = U(r) + u$$
$$v' = V(r) + v$$
$$w' = W(r,z) + w \tag{5}$$
$$p' = P(r,z) + p$$

where u, v, w, and p are the perturbations in the velocities and the pressure. These quantities are assumed to have a helical wave form:

$$\{u, v, w, p\} = \{iF(r), G(r), H(r), P(r)\}\, e^{i(\alpha z + n\theta - \omega t)} \tag{6}$$

Here, F, G, H, and P are the perturbations amplitudes which are functions of radial position only, α is the wave number in the axial direction, n is the wave number in the azimuthal direction, and ω is the frequency of oscillation. For a single valued solution, n must be an integer. The case of n equal to zero corresponds to that of axisymmetric disturbances and positive and negative integers represent different directions of propagation. For positive n, the helical wave spirals in the same direction as the circulatory motion of the vortex while a negative value indicates that the wave spirals opposite to the circulatory motion.

Substituting into the equations of motion and neglecting the second order terms, we obtain the small disturbance equations

continuity

$$\frac{\partial u}{\partial r} + \frac{u}{r} + \frac{1}{r}\frac{\partial v}{\partial \theta} + \frac{\partial w}{\partial z} = 0, \tag{7}$$

r-momentum

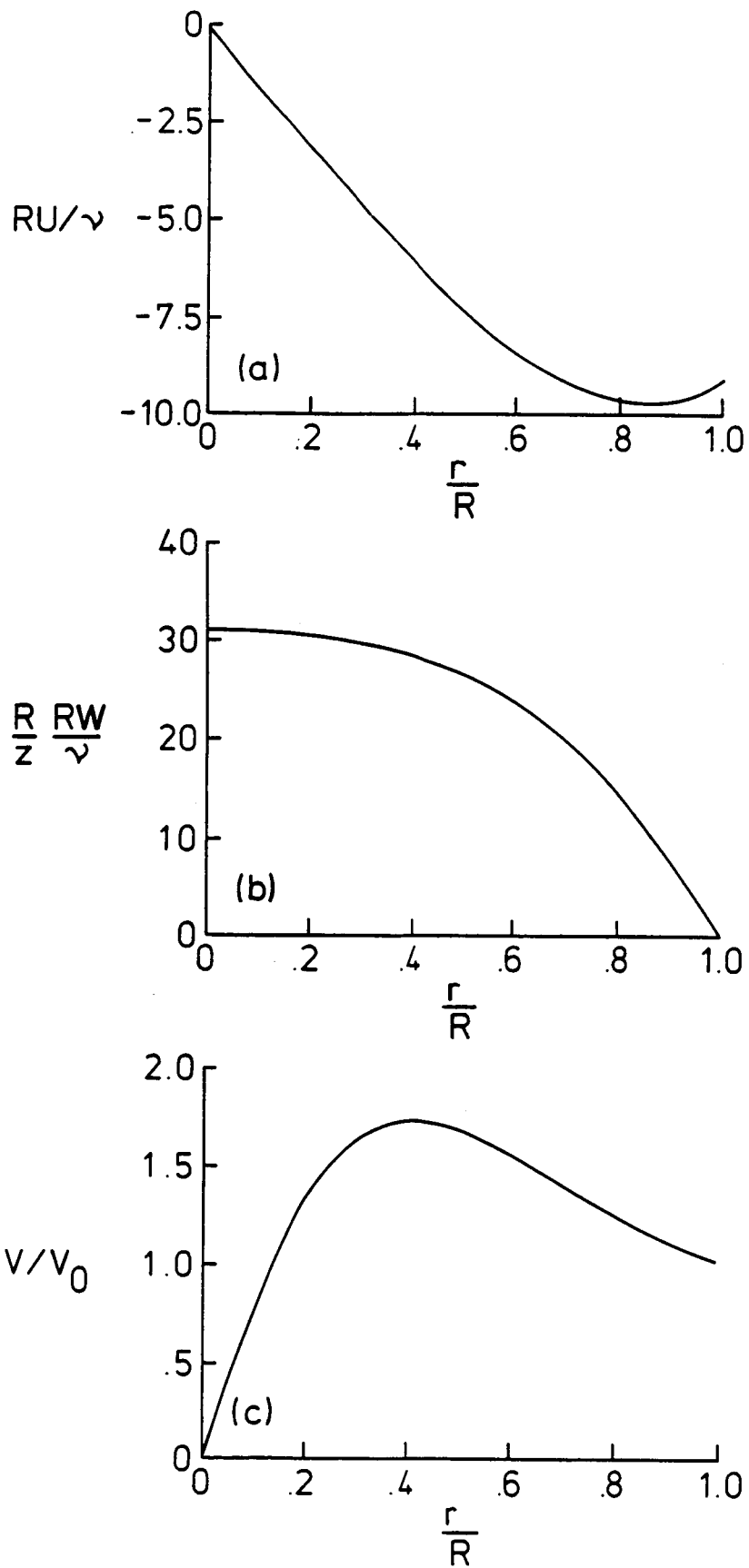$$\frac{\partial u}{\partial t} + U\frac{\partial u}{\partial r} + u\frac{dU}{dr} + \frac{V}{r}\frac{\partial u}{\partial \theta} + W\frac{\partial u}{\partial z} - \frac{2Vv}{r} = -\frac{1}{\rho}\frac{\partial p}{\partial r}$$

$$+ \nu \left[\frac{\partial^2 u}{\partial r^2} + \frac{1}{r}\frac{\partial u}{\partial r} + \frac{1}{r^2}\frac{\partial^2 u}{\partial \theta^2} + \frac{\partial u^2}{\partial z^2} - \frac{u}{r^2} - \frac{2}{r^2}\frac{\partial v}{\partial \theta}\right], \tag{8}$$

θ-momentum

$$\frac{\partial v}{\partial t} + U\frac{\partial v}{\partial r} + u\frac{dV}{dr} + \frac{V}{r}\frac{\partial v}{\partial \theta} + W\frac{\partial v}{\partial z} + \frac{Vu}{r} + \frac{vU}{r} = -\frac{1}{\rho r}\frac{\partial p}{\partial \theta}$$

$$+ \nu \left[\frac{\partial^2 v}{\partial r^2} + \frac{1}{r}\frac{\partial v}{\partial r} + \frac{1}{r^2}\frac{\partial^2 v}{\partial \theta^2} + \frac{\partial^2 v}{\partial z^2} - \frac{v}{r^2} + \frac{2}{r^2}\frac{\partial u}{\partial \theta}\right], \tag{9}$$

z-momentum

$$\frac{\partial w}{\partial t} + u \frac{\partial W}{\partial r} + U \frac{\partial w}{\partial r} + \frac{V}{r} \frac{\partial w}{\partial \theta} + W \frac{\partial w}{\partial z} + w \frac{\partial W}{\partial z} = - \frac{1}{\rho} \frac{\partial p}{\partial z}$$

$$+ \nu \left[\frac{\partial^2 w}{\partial r^2} + \frac{1}{r} \frac{\partial w}{\partial r} + \frac{1}{r^2} \frac{\partial^2 w}{\partial \theta^2} + \frac{\partial^2 w}{\partial z^2} \right] . \tag{10}$$

The boundary conditions at the outer wall are

$$\text{at } r = R_0 \qquad\qquad \begin{aligned} u &= 0 \\ v &= 0 \\ w &= 0 \\ p &= 0 \end{aligned} \tag{11}$$

and on the centerline[1]

$$\text{at } r = 0 \qquad\qquad \begin{aligned} \lim_{r \to 0} \frac{\partial \vec{q}}{\partial \theta} &= 0 \\[2mm] \lim_{r \to 0} \frac{\partial p}{\partial \theta} &= 0 \end{aligned} \tag{12}$$

where $\vec{q}$ is the total velocity vector.

Substitution of the perturbation Eq. (6) into the linearized momentum equations results in four equations for the disturbance amplitudes. These equations in non-dimensional form are:

continuity

$$F' + \frac{F}{r} + \frac{nG}{r} + \alpha H = 0 \tag{13}$$

---

[1] We are very grateful to Dr. M. Y. Hussaini of the Institute for Computer Applications in Science and Engineering for mentioning this simple yet very powerful way of determining the boundary conditions on the centerline.

r-momentum

$$-\frac{iF''}{Re} + i\left[U - \frac{1}{Re\ r}\right]F' + \left[\omega + i\frac{dU}{dr} - \frac{nV}{r} - \alpha W + \frac{i}{Re}\left(\frac{n^2}{r^2}\right)\right.$$

$$\left.+ \alpha^2 + \frac{1}{r^2}\right)\right]F + \left[\frac{i2n}{Re\ r^2} - \frac{2V}{r}\right]G + P' = 0 \qquad (14)$$

θ-momentum

$$-\frac{1}{Re}G'' + \left[U - \frac{1}{Re\ r}\right]G' + \left[-i\omega + \frac{inV}{r} + i\alpha W + \frac{U}{r} + \frac{1}{Re}\left(\frac{n^2}{r^2}\right.\right.$$

$$\left.\left.+ \alpha^2 + \frac{1}{r^2}\right)\right]G + \left[i\frac{dV}{dr} + \frac{2n}{Re\ r^2} + \frac{iV}{r}\right]F + \frac{inP}{r} = 0 \qquad (15)$$

z-momentum

$$-\frac{1}{Re}H'' + \left[U - \frac{1}{Re\ r}\right]H' + \left[-i\omega + i\alpha W + \frac{inV}{r} + \frac{\partial W}{\partial z} + \frac{1}{Re}\left(\frac{n^2}{r^2}\right.\right.$$

$$\left.\left.+ \alpha^2\right)\right]H + i\frac{\partial W}{\partial r}F + i\alpha P = 0 \qquad (16)$$

where Re is the Reynolds number based on pipe radius Ro and prime denotes differentiation with respect to the radial coordinate. The boundary conditions at $r = R_0$ are:

$$F(R_0) = G(R_0) = H(R_0) = 0.$$

$$P'(R_0) = \text{Normal momentum at } R_0.$$

The derivation of conditions on the centerline is not simple or straight forward and deserves a fuller explanation. In expanding the conditions (12), we need to consider only the perturbation part of the velocity since the mean velocity profile is independent of the azimuthal direction.

14

Assuming that the total perturbation velocity field is represented by $\vec{v}$, we have:

$$\frac{\partial \vec{v}}{\partial \theta} = \frac{\partial}{\partial \theta} \left(u \, \vec{e}_r + v \, \vec{e}_\theta + w \vec{e}_z \right)$$

or

$$\lim_{r \to 0} \frac{\partial \vec{v}}{\partial \theta} = \frac{\partial u}{\partial \theta} \vec{e}_r + u \frac{d\vec{e}_r}{d\theta} + \frac{\partial v}{\partial \theta} \vec{e}_\theta + v \frac{d\vec{e}_\theta}{d\theta} + \frac{\partial w}{\partial \theta} \vec{e}_z + w \frac{d\vec{e}_z}{d\theta} \; .$$

But in cylindrical coordinates (Appendix 2, Batchelor [1967])

$$\frac{d\vec{e}_z}{d\theta} = 0$$

$$\frac{d\vec{e}_r}{d\theta} = \vec{e}_\theta$$

$$\frac{d\vec{e}_\theta}{d\theta} = -\vec{e}_r \quad .$$

Substituting for the velocities from (6) and evaluating the derivatives, we deduce

$$\lim_{r \to 0} \frac{\partial \vec{v}}{\partial \theta} = (-nF - G) \, \vec{e}_r + (iF + inG) \, \vec{e}_\theta + inH \, \vec{e}_z = 0$$

In order for the equality to hold, each component of the resultant vector must be zero. Similarly, the limiting process applied to the pressure leads to

$$\lim_{r \to 0} \frac{\partial P}{\partial \theta} = inP .$$

In summary, we have at $r = 0$,

$$
\begin{aligned}
nF + G &= 0 \\
F + nG &= 0 \\
nH &= 0 \\
nP &= 0 .
\end{aligned}
\tag{17}
$$

The above conditions depend on the value of the azimuthal wave number, n, such that

$$
\text{If } n = 0 \qquad
\begin{aligned}
F(0) &= G(0) = 0 \\
H(0) &\text{ \& } P(0) \text{ are finite}
\end{aligned}
\tag{18}
$$

$$
\text{If } n = \pm 1 \qquad
\begin{aligned}
F(0) &\pm G(0) = 0 \\
H(0) &= P(0) = 0
\end{aligned}
\tag{19}
$$

$$
\text{If } |n| > 1 \qquad
\begin{aligned}
F(0) &= G(0) = 0 \\
H(0) &= P(0) = 0 .
\end{aligned}
\tag{20}
$$

Due to the extreme complexity of the Eqs. (13)-(16), no attempt was made to reduce the above system into a single, sixth order ordinary differential equation. We believe that this would be of no great value in solving the problem numerically.

2.3 Proposed Numerical Scheme

The system of Eqs. (13)-(16) can be represented in a compact vector

form as:

$$L(\alpha)\ \vec{A} = 0 \qquad\qquad (21)$$

with

$$\vec{A} = \begin{Bmatrix} F \\ G \\ H \\ P \end{Bmatrix}$$

and

$$L(\alpha) = D_0 \alpha^2 + D_1 \alpha + D_2 \qquad\qquad (22)$$

D_0, D_1, and D_2 are discretized versions of the differential operator matrices. This type of operator (where the eigenvalue appears nonlinearly) is called a Lambda-matrix (Lancaster [1966]).

It was decided to use the method of Bridges and Morris [1984] to solve this nonlinear matrix eigenvalue problem. The advantages of choosing their method are threefold. (1) It is a global eigenvalue scheme. This is clearly an advantage because the availability of an initial guess for a shooting method is not needed. Of course these global eigenvalues can be refined until a desired accuracy is reached, by any local iterative scheme once they are obtained. (2) The method is robust. In some cases infinite eigenvalues are encountered, and in such instances, the remainder of the eigenvalues are obtained without any difficulty. (3) Most of the subroutines needed are available in any mathematical software library. In particular this is true for the complex version of the QZ routine which is the heart of the present scheme.

The method can be described quite briefly. First the discrete operator $L(\alpha)$ is factored such that

$$L(\alpha) = [D_0\alpha + D_0 Y + D_1] [I\alpha - Y] + D_0 Y^2 + D_1 Y + D_2. \qquad (23)$$

where I is the identity matrix and the Y matrix is referred to as the right solvent (Gantmacher, 1959). Now, in order that (23) be consistent with (22), one must have

$$[I\ \alpha - Y] = 0 \qquad (24)$$

or

$$[D_{0\alpha} + D_0 Y + D_1] = 0. \qquad (25)$$

Multiplying Eq. (25) by α and subtracting from Eq. (22) yields

$$\alpha D_0 Y = D_2.$$

Since α is an arbitrary scalar multiplication factor, in general

$$\alpha D_0 Y \neq D_2 \qquad (26)$$

and Eq. (24) must be satisfied. Therefore from the above factorization, it is obvious that what we must find is the root matrix of the matrix polynomial

$$D_0 Y^2 + D_1 Y + D_2 = 0$$

This can easily be accomplished through an iterative procedure. Then a subset of the eigenvalues of $L(\alpha)$ is given by the set of eigenvalues of Y obtained from (24). A flow chart of the numerical scheme is given in Fig. 4

18
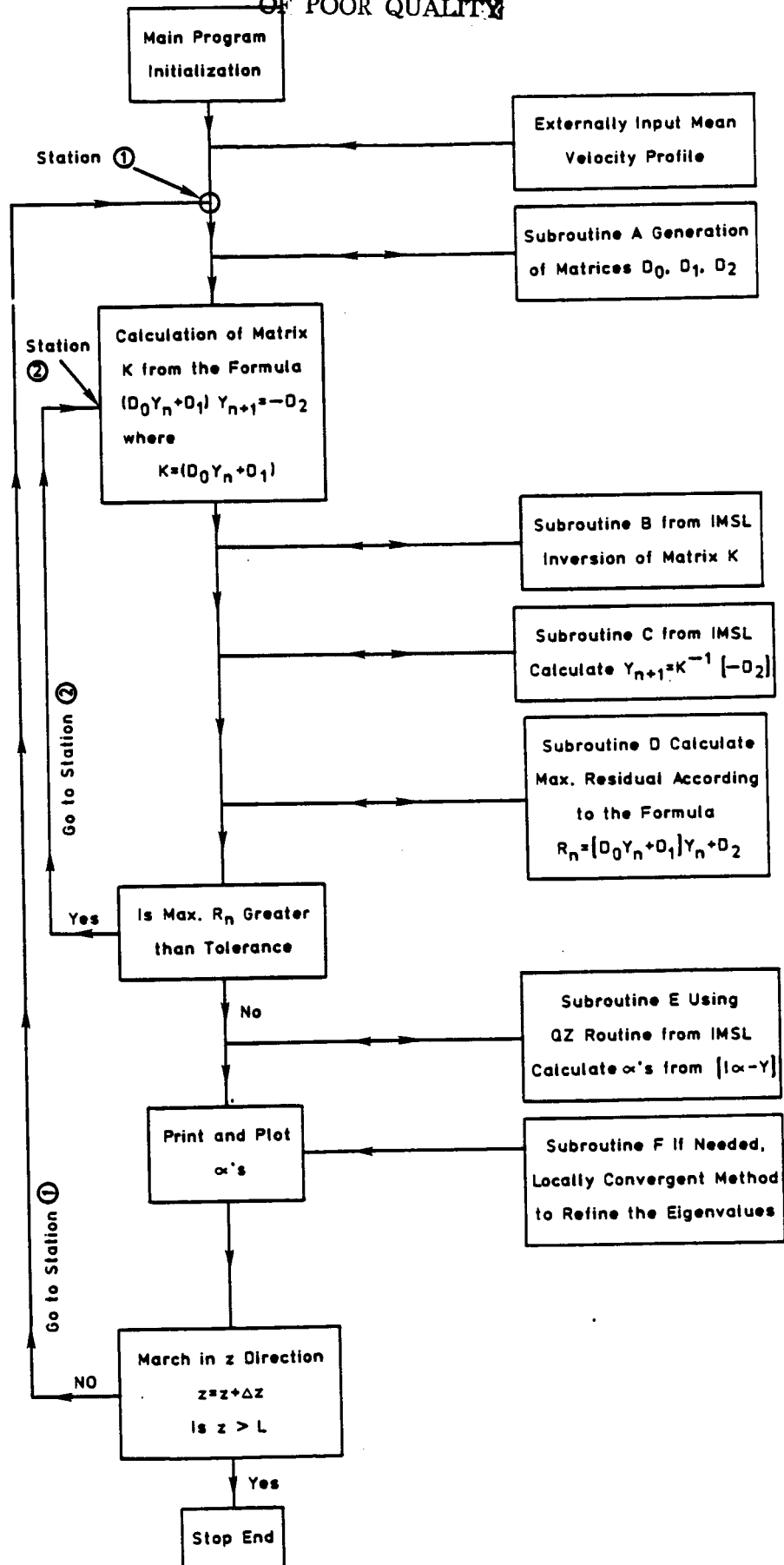
Fig. 4. Flow chart for the numerical scheme used in this investigation.

which shows the steps needed to find a single solution. For a further description of the method and its implementation, the reader is referred to the paper of Bridges and Morris [1984].

3. TEST PROBLEMS

3.1 Calculation of the Matrices and Testing of the Algorithm

Prior to the implementation of the difference scheme, the algorithm was checked using a problem with known eigenvalues as a test case. This problem was taken from Gregory and Karney [1969], and along with its eigenvalues is given in Table 1. The correct eigenvalues were obtained and are tabulated in Table 2. Finding the right values assured us that the coding was free of logical error.

It is well known that spectral methods are efficient methods for solving eigenvalue problems. Metcalfe and Orszag [1973] have shown that for calculation of the linear stability of these types of swirling flows spectral calculations are very accurate. Because there are no results available with which to compare our results (for the stability of velocity profiles due to Donaldson and Sullivan), it seemed desirable to solve the above matrix eigenvalue problem using two independent formulations. It was decided that in order to obtain an approximate estimate of the eigenvalues, finite differencing of the operator matrices would be employed. These approximate values could then be used to cross check the eigenvalues found by a spectral method. This was done but peripheral problems were encountered relating to difficulties with convergence (actually, lack of convergence) of the solution. A new test problem was chosen in order to check the accuracy of the finite difference approximation. This problem is that of Poiseuille flow in concentric cylinders and is described in section 3.2.

After careful examination, we found that the lack of convergence of the

Table 1. Matrix used as a test problem.

$$
\begin{bmatrix}
5 + 9i & 5 + 5i & -6 - 6i & -7 - 7i \\
3 + 3i & 6 + 10i & -5 - 5i & -6 - 6i \\
2 + 2i & 3 + 3i & -1 + 3i & -5 - 5i \\
1 + i & 2 + 2i & -3 - 3i & 4i
\end{bmatrix}
$$

Eigenvalues:

$$\lambda_1 = 1 + 5i$$

$$\lambda_2 = 2 + 6i$$

$$\lambda_3 = 3 + 7i$$

$$\lambda_4 = 4 + 8i$$

Table 2. Calculated eigenvalues using the method of Bridges and Morris.

REAL C	IMAG C
2.000000	6.000000
4.000000	8.000000
3.000000	7.000000
1.000000	5.000000

difference solution was dependent on a number of factors (see Appendix A) namely, boundary conditions on the centerline, number of grid points, and second order accuracy. Therefore, a model problem had to be chosen so that an analysis of some of the above mentioned factors was possible in a short time and at the same time the problem had to have been solved by other workers to enable a comparison.

The temporal stability of Poiseuille flow in an annulus was picked to be the model problem used for testing.

3.2 Temporal Stability of Poiseuille Flow in Concentric Cylinders

For this problem there are no effects of the centerline boundary conditions because the no-slip condition applies at both boundaries. Furthermore, the continuity equation along with the pressure terms were staggered and evaluated at the set of points $\{r_{j+1/2}\}$ while the momentum equations were evaluated at the set of points $\{r_j\}$. Here the index j takes on values between zero and N, where N specifies the total number of nodes. The grid points were distributed uniformly over the gap distance and no attempt was made to concentrate or stretch them. Therefore, the only factors influencing accuracy that we had to deal with were the number of grid points and the second order central differencing scheme.

3.2a Mean Velocity Profile

The mean velocity profile for Poiseuille flow in an annulus is

$$U = 0$$
$$V = 0$$
$$W = W(r)$$

where, in non-dimensional form, W is given by

$$\frac{W}{W_M} = \frac{1 - r^2 + r_M^2 \, \ell n \, r^2}{1 - r_M^2 + r_M^2 \, \ell n \, r_M^2} .$$ (27)

The non-dimensionalization has been done with respect to the maximum velocity and the half gap distance (see equations 9B and 4B in Appendix B). A detailed derivation of this velocity profile can be found in Appendix B.

3.2b Governing Equations

It is obvious from the form of the mean velocity profile that the equivalent of Eqs. (13) - (16) is much simpler due to the absence of both radial and tangential velocity components. The equations are:

continuity

$$\frac{F}{r} + F' + \frac{nG}{r} + \alpha H = 0$$ (28)

r-momentum

$$-\frac{i}{Re} F'' - \frac{i}{Re \, r} F' + \left[\omega - \alpha W + \frac{i}{Re} \left(\frac{n^2}{r^2} + \alpha^2 + \frac{1}{r^2} \right) \right] F + \frac{i2n}{Re \, r^2} G + P' = 0$$ (29)

θ-momentum

$$-\frac{1}{Re} G'' - \frac{1}{Re \, r} G' + \left[-i\omega + i\alpha W + \frac{1}{Re} \left(\frac{n^2}{r^2} + \alpha^2 + \frac{1}{r^2} \right) \right] G$$

$$+ \frac{2n}{Re \, r^2} F + \frac{in}{r} P = 0$$ (30)

z-momentum

$$-\frac{1}{Re} H'' - \frac{1}{Re\ r} H' + \left[-i\omega + i\alpha W + \frac{1}{Re}\left(\frac{n^2}{r^2} + \alpha^2\right)\right] H + i\frac{dW}{dr} F + i\alpha P = 0. \quad (31)$$

Employing a second order accurate central differencing technique for the derivatives, the discretized equations are

$$\frac{F_j + F_{j-1}}{2r_{j-1/2}} + \frac{F_j - F_{j-1}}{\Delta r} + \frac{n}{2r_{j-1/2}}(G_j + G_{j-1}) + \frac{\alpha}{2}(H_j + H_{j-1})$$
$$+ \gamma\omega P_j^* = 0 \quad (32)$$

$$-\frac{i}{Re}\left[\frac{F_{j+1} - 2F_j + F_{j-1}}{\Delta r^2}\right] + \frac{-i}{Re\ r_j}\left[\frac{F_{j+1} - F_{j-1}}{2\Delta r}\right] + \left[\omega - \alpha W_j\right.$$
$$+ \frac{i}{Re}\left(\frac{n^2+1}{r_j^2} + \alpha^2\right)\right] F_j + \frac{i2n}{Re\ r_j^2} G_j + \left[\frac{P_{j+1}^* - P_j^*}{\Delta r}\right] = 0 \quad (33)$$

$$-\frac{1}{Re}\left[\frac{G_{j+1} - 2G_j + G_{j-1}}{\Delta r^2}\right] + \frac{-1}{Re\ r_j}\left[\frac{G_{j+1} - G_{j-1}}{2\Delta r}\right] + \left[-i\omega + i\alpha W_j\right.$$
$$+ \frac{1}{Re}\left(\frac{n^2+1}{r_j^2} + \alpha^2\right)\right] G_j + \frac{2n}{Re\ r_j^2} F_j + \frac{in}{2r_j}\left[P_{j+1}^* + P_j^*\right] = 0 \quad (34)$$

$$-\frac{1}{R_e}\left[\frac{H_{j+1} - 2H_j + H_{j-1}}{\Delta r^2}\right] + \frac{-1}{Re\ r_j}\left[\frac{H_{j+1} - H_{j-1}}{2\Delta r}\right] + \left[-i\omega + i\alpha W_j\right.$$
$$+ \frac{1}{Re}\left(\frac{n^2}{r_j^2} + \alpha^2\right)\right] H_j + i\left(\frac{dW}{dr}\right)_j F_j + \frac{i\alpha}{2}\left(P_{j+1}^* + P_j^*\right) = 0 \quad (35)$$

where asterisks denote mid-cell values. The boundary conditions

24

$$\text{No slip} \quad \begin{cases} G(a) \equiv G_0 = 0 \\ H(a) \equiv H_0 = 0 \\ G(b) \equiv G_N = 0 \\ H(b) \equiv H_N = 0 \end{cases}$$

$$\text{No penetration} \quad \begin{cases} F(a) \equiv F_0 = 0 \\ F(b) \equiv F_N = 0 \end{cases}$$

where a and b are the radius of inner and outer walls, respectively. Note that the term $\gamma \omega P_j^*$ has been added in Eq. (32). This makes the coefficient matrix of omega non-singular. Otherwise it would have N rows with zero entries. This term is obtained by adding $\gamma \dfrac{\partial P}{\partial t}$ to the continuity equation, which is why it is called an artificial compressibility factor (Malik and Poll [1985]). The parameter, γ, is chosen to be a very small number and, in the present case, a value of 10^{-12} was used. This term causes large values for some of the unimportant eigenvalues; however, its affect on the desired eigenvalues is negligible. Experimentation with the value of γ with the present code indicated that this was indeed the case.

The above system can be expressed in the following way:

$$[K-\omega M] \, [X] = 0$$

where

$$X = \begin{bmatrix} F \\ G \\ H \\ P \end{bmatrix} .$$

The eigenvalues are then obtained from the requirement:

$$[M^{-1} K - \omega I] = 0 \ .$$

Here we have made sure that M^{-1} exists by adding the term $\gamma \omega P_j^*$ (as mentioned previously) to the continuity equation. The remaining procedure is straight forward and simple. Any Gauss-Jordan algorithm with pivoting strategy can be employed to invert matrix, M, and then using a standard QR routine, the eigenvalues of the matrix M^{-1} K can be evaluated.

3.3 Results

The above system of equations and boundary conditions were solved on the vector processor computer (VPS-32) at NASA Langley Research Center for the narrow gap case. It is well known that as the gap distance shrinks, for fixed inner radius, the eigenvalues approach those of plane Poiseuille flow. Therefore, the narrow gap calculation was performed so that the results could be compared to the accurate eigenvalues of plane-Poiseuille flow reported by Orszag [1971]. All of the calculations reported here correspond to the axisymmetric type of disturbances where the azimuthal wavenumber, n, is zero, and the gap distance is 0.01. The results of these calculations, along with Orszag's results, are tabulated in Table 3.

Initially, the calculations were started with 20 grid points and no satisfactory results were obtained. That suggested that the number of grid points had to be increased. After increasing the grid points, many of the eigenvalues found by Orszag were obtained, but with only modest accuracy. The number of nodes was increased further by fifteen percent from 140 to 160. However, improvement of the accuracy of the eigenvalues was slow with the side effect of almost doubling the cost of each computer run.

We concluded that a second order accurate finite difference scheme is

Table 3. Comparison of present calculations with those of Orszag [1971].

ORSZAG RESULTS   PRESENT CALCULATIONS

Mode Number	Symmetric (S) Anti-symmetric (A)	Eigenvalue λ	N = 80	N = 140	N = 160
1	S	0.23752649 + 0.00373967i	0.2405217 - 0.0016056i	0.2384168 + 0.0018922i	0.2381987 + 0.0023166i
2	A	0.96463092 - 0.03516728i	0.9651255 - 0.0351781i	0.9647865 - 0.0351700i	0.9647481 - 0.0351693i
3	S	0.96464251 - 0.03518658i	0.9651527 - 0.0351972i	0.9648140 - 0.0351894i	0.9647756 - 0.0351887i
4	A	0.27720434 - 0.05089873i	0.2789518 - 0.0606954i	0.2775705 - 0.0541611i	0.2774654 - 0.0533999i
5	A	0.93631654 - 0.06320150i	0.9379097 - 0.0632441i	0.9368291 - 0.0632111i	0.9367073 - 0.0632086i
6	S	0.93635178 - 0.06325157i	0.9379567 - 0.0632916i	0.9368758 - 0.0632598i	0.9367540 - 0.0632574i
7	A	0.90798305 - 0.09122274i	0.9113144 - 0.0913343i	0.9090559 - 0.0912447i	0.9088024 - 0.0912384i
8	S	0.90805633 - 0.09131286i	0.911397 - 0.0914176i	0.9091381 - 0.0913325i	0.9088845 - 0.0913267i
9	A	0.87962729 - 0.11923285i	0.8853475 - 0.1194678i	0.8814657 - 0.1192756i	0.8810316 - 0.1192628i
10	S	0.87975570 - 0.11937073i	0.8854844 - 0.1195894i	0.8816011 - 0.1194086i	0.8811670 - 0.1193970i
11	A	0.34910682 - 0.12450198i	0.3440515 - 0.1370131i	0.3471288 - 0.1284677i	0.3475660 - 0.1275229i
12	S	0.41635102 - 0.13822652i	0.4125554 - 0.1559114i	0.4145538 - 0.1439037i	0.4149275 - 0.1425552i
13	A	0.8512458 - 0.1472339i	0.8600167 - 0.1476643i	0.8540568 - 0.1473077i	0.8533928 - 0.1472852i
14	S	0.8514494 - 0.1474256i	0.8602256 - 0.1478230i	0.8542652 - 0.1474896i	0.8536014 - 0.1474695i
15	A	0.8228350 - 0.1752287i	0.8353291 - 0.1759456i	0.8268277 - 0.1753460i	0.8258837 - 0.1753094i
16	S	0.8231370 - 0.1754781i	0.8356296 - 0.1761363i	0.8271311 - 0.1755779i	0.8261877 - 0.1755457i
17	A	0.1900592 - 0.1828219i	0.1807736 - 0.1806230i	0.1872334 - 0.1820237i	0.1879118 - 0.1822063i
18	S	0.794388 - 0.2032211i	0.8112918 - 0.2043352i	0.7997763 - 0.2033959i	0.7985013 - 0.2033405i
19	A	0.794818 - 0.2035293i	0.8117032 - 0.2045485i	0.8001999 - 0.2036757i	0.7989274 - 0.2036271i
20	S	0.532045 - 0.2064651i	0.5221059 - 0.2337831i	0.5277449 - 0.2149848i	0.5286694 - 0.2129308i
21	A	0.474901 - 0.2087311i	0.4630123 - 0.2306847i	0.4702797 - 0.2154029i	0.4713100 - 0.2137817i
22	S	0.76588 - 0.231191i	0.7879092 - 0.2328609i	0.7728925 - 0.2314567i	0.7712383 - 0.2313748i
23	A	0.76649 - 0.231591i	0.7884593 - 0.2330819i	0.7734708 - 0.2317853i	0.7718165 - 0.2317206i
24	S	0.36850 - 0.238821i		0.3623601 - 0.2411800i	0.3638184 - 0.2405802i
25	A	0.73741 - 0.258721i		0.7461630 - 0.2594469i	0.7440472 - 0.2592791i
26	S	0.73812 - 0.259691i		0.7469602 - 0.2599393i	0.7448754 - 0.2598138i
27	A	0.63672 - 0.259881i		0.6302985 - 0.2718773i	0.6316636 - 0.2689504i
28	A	0.38399 - 0.265111i		0.3767189 - 0.2671028i	0.3784530 - 0.2665755i
29	S	0.58721 - 0.267161i		0.5802618 - 0.2770060i	0.5817944 - 0.2745900i
30	A	0.71232 - 0.285511i		0.7201144 - 0.2863899i	0.7180414 - 0.2860955i
31	S	0.51292 - 0.286631i		0.5037606 - 0.2932499i	0.5059024 - 0.2915821i
32	S	0.70887 - 0.287651i		0.7203721 - 0.2880952i	0.7176814 - 0.2882755i

α = 1, Re = 10000.   α = 1, Re = 10000.

only accurate enough for obtaining rough estimates for this type of global eigenvalue calculation and, therefore, the method was abandoned. Hence, a spectral method has been selected.

4. SPECTRAL METHOD

A Chebyshev collocation approach was chosen. Truncated series of Chebyshev polynomials were employed in expanding the flow variables. Because the problem is non-periodic, this form of expansion has the advantage of eliminating terminal discontinuities. In addition, the expansion exhibits a rapid convergence rate as the number of terms increases and clusters the collocation points (see Eq. 43) near the boundaries.[2] The Chebyshev polynomials are defined on an interval of (-1, 1) by

$$T_k(\xi) = \cos [k \cos^{-1}\xi] \tag{36}$$

Because the physical range in this problem is (0, 1), a simple transformation is made from the physical variable r to a transform variable ξ by

$$\xi = 1 - 2 r \tag{37}$$

where

$$-1 < \xi < 1.$$

The mean velocity profile must be transformed similarly in order to be compatible. A sample case is shown in Figs. 5a-5c which correspond to Figs. 1a-1c.

---

[2]For a thorough exposition of Chebyshev approach, the reader is urged to consult the excellent treatises of Gottlieb and Orszag [1977], Gottlieb, Hussaini and Orszag [1983], and Hussaini, Streett and Zang [1984].
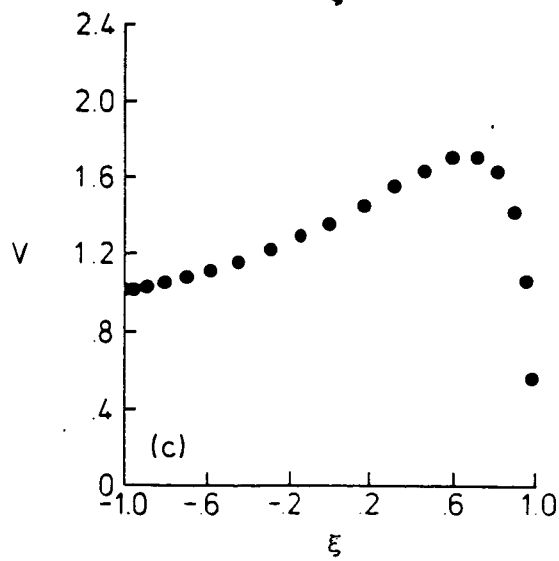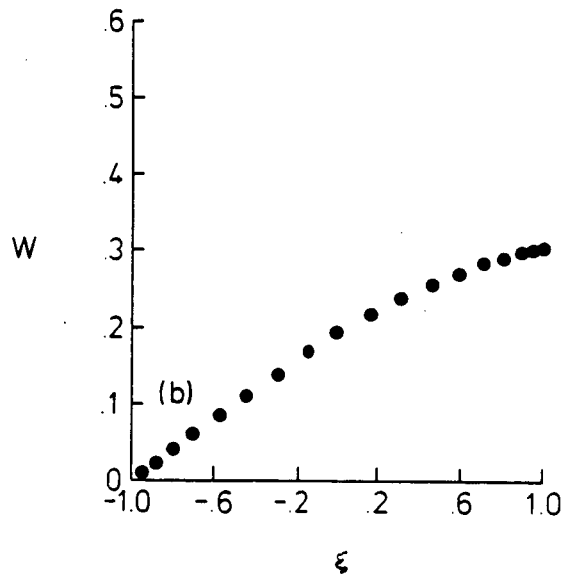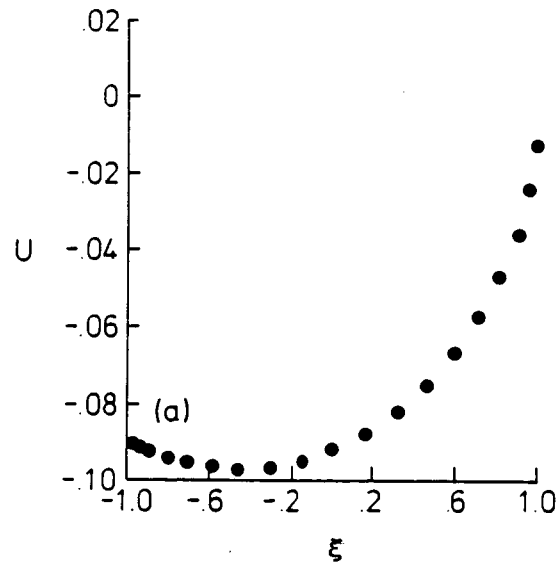
Fig. 5. a) Transformed radial velocity, b) Transformed axial velocity, and c) Transformed tangential velocity.

Let

$$\xi = \cos \theta,$$

then

$$T_k(\xi) = \cos k\theta. \qquad (38)$$

The periodic nature of Chebyshev polynomials is apparent from the above identity. The governing equations are then satisfied exactly at collocation points which are the roots of the Nth degree Chebyshev polynomial $T_N(\xi)$. It must be mentioned that it is only at this set of points that one obtains spectral accuracy (Gottlieb and Orszag [1977]). These points are defined by

$$r_j = \cos \frac{\pi j}{N} \qquad (39)$$

where

$$j = 0, 1, 2, \ldots, N$$

with $j = 0$ and $j = N$ corresponding to the centerline and wall boundary conditions, respectively.

An interpolant polynomial is constructed in terms of the values of the variable at the collocation points with the help of truncated Chebyshev series. Next, the first and second derivative of the variable are explicitly determined using the above interpolant such that (as an example we present only variable $F(\xi)$ since the extension to other variables is very obvious)

$$\frac{dF}{d\xi}\bigg|_j = \sum_{k=0}^{N} A_{jk} F_k \qquad (40)$$

$$\frac{d^2F}{d\xi}\bigg|_j = \sum_{k=0}^{N} B_{jk} F_k \qquad (41)$$

$$j = 0,1,\ldots,N$$

where A_{jk} and B_{jk} are the elements of the derivative matrices and are given by Gottlieb et al. [1983] as

$$A_{jk} = \frac{\overline{C_j}}{\overline{C_k}} \frac{(-1)^{k+j}}{\xi_j - \xi_k} \quad (j \neq k) \qquad (42)$$

$$A_{jj} = - \frac{\xi_j}{2(1 - \xi_j^2)}$$

$$A_{oo} = \frac{2N^2 + 1}{6} = - A_{NN}$$

with $\qquad \overline{C}_o = \overline{C}_N, \ \overline{C}_j = 1, \ (1 < j < N-1),$

and

$$B = AA = A^2 \qquad (43)$$

It is clear that any higher derivative can be obtained by utilizing relation (43).

From our transformation, we obtain

$$\frac{1}{r} = \frac{2}{1 - \xi}, \quad \frac{1}{r^2} = \frac{4}{(1-\xi)^2}$$

and

$$\frac{d}{dr} = \frac{d\xi}{dr}\frac{d}{d\xi} = -2\frac{d}{d\xi} = S_1\frac{d}{d\xi}$$

$$\frac{d^2}{dr^2} = \frac{d}{dr}(\frac{d}{dr}) = 4\frac{d^2}{d\xi^2} = S_2\frac{d^2}{d\xi^2} \, .$$

Here S_1 and S_2 are the scaling factors involved from the transformation.

Writing the governing equations in terms of the new variable and evaluating at the collocation points, we have

Continuity:

$$S_1 \sum_{k=0}^{N} A_{jk} F_k + (\frac{2}{1-\xi_j}) F_j + (\frac{2n}{1-\xi_j}) G_j + \alpha H_j = 0 \qquad (44)$$

r-momentum:

$$S_2 \sum_{k=0}^{N} B_{jk} F_k + [\frac{2}{1-\xi_j} - Re \; U_j] S_1 \sum_{k=0}^{N} A_{jk} F_k + [iRe_\omega - $$

$$ReS_1 \frac{dU}{d\xi}\Big|_j - \frac{i2Re \; n \; V_j}{1 - \xi_j} - (\frac{4(n^2+1)}{(1-\xi_j)^2})] F_j - [\frac{4(2n)}{(1-\xi_j)^2} + $$

$$\frac{2(i2Re \; V_j)}{1-\xi_j}] G_j + iReS_1 \sum_{k=0}^{N} A_{jk} P_k - \alpha iRe \; W_j F_j - $$

$$\alpha^2 F_j = 0 \qquad (45)$$

32

θ-momentum:

$$-\left[iReS_1 \left.\frac{dV}{d\xi}\right|_j + \frac{4(2n)}{(1-\xi_j)^2} + \frac{2(iRe\ V_j)}{(1-\xi_j)}\right] F_j + S_2 \sum_{k=0}^{N} B_{jk}\ G_k$$

$$+ \left[\frac{2}{1-\xi_j} - Re\ U_j\right] S_1 \sum_{k=0}^{N} A_{jk}\ G_k + \left[iRe\omega - \frac{2(iRen\ V_j)}{1-\xi_j} - \right.$$

$$\left.\frac{2(reU_j)}{1-\xi_j} - \frac{4(n^2+1)}{(1-\xi_j)^2}\right] G_j - \frac{2(iRe\ n)}{1-\xi_j} P_j - \alpha iRe\ W_j\ G_j - \alpha^2 G_j = 0 \quad (46)$$

Z-momentum

$$-iRe\ S_1 \left.\frac{\partial W}{\partial \xi}\right|_j F_j + S_2 \sum_{k=0}^{N} B_{jk}\ H_k + \left[\frac{2}{1-\xi_j} - ReU_j\right]$$

$$S_1 \sum_{k=0}^{N} A_{jk}\ H_k + \left[iRe\omega - \frac{2(iRe\ n\ V_j)}{1-\xi_j} - Re \left.\frac{\partial W}{\partial Z}\right|_j - \right.$$

$$\left.\frac{4(n^2)}{(1-\xi_j)^2}\right] H_j - i\alpha Re\ W_j\ H_j - i\alpha Re\ P_j - \alpha^2\ H_j = 0 \quad (47)$$

with the boundary conditions

at $\xi = -1$ $F(-1) = G(-1) = H(-1) = 0$

for all n $\left.\frac{\partial P}{\partial \xi}\right|_{\xi = -1} = $ Normal momentum
                              evaluated at $\xi = -1$ (48)

at $\xi = 1$

If n = 0 $F(1) = G(1) = 0$

                    H(1) & P(1) are finite   (49)

33

If $n = \pm1$
$$F(1) \pm G(1) = 0$$
$$H(1) = P(1) = 0 \qquad (50)$$

If $|n| > 1$
$$F(1) = G(1) = 0$$
$$H(1) = P(1) = 0. \qquad (51)$$

REFERENCES

Adams, G. N. and Gilmore, D.C. 1972. Some observations of vortex core structure. _Canadian Aeronautics and Space Journal_, 18, 159-162.

Batchelor, G. K. 1964. Axial flow in the trailing line vortices. _J. Fluid Mech_. 20, 645-658.

Batchelor, G. K. 1967. _An introduction to fluid dynamics_. Cambridge University Press, Cambridge.

Betchov, R. 1965. On the curvature and torsion of a vortex filament. _J. Fluid Mech_. 22, 471-479.

Bridges, T. J. and Morris, P. J. 1984. Differential eigenvalues problems in which the parameter appears nonlinearly. _J. Comp. Phys. 55_, No. 3, 437-460.

Donaldson, C. P. and Sullivan, R. D. 1960. Examination of the solutions of the Navier-Stokes equations for a class of three-dimensional vortices, Part I: Velocity distributions for steady motion. Aeronautical Research Associates of Princeton, AFOSR TN 60-1227.

Duck, P. W. and Foster, M. R. 1980. The inviscid stability of a trailing line vortex. _Z. angew. Math Phys_. 31, 523-530.

Gantmacher, F. R. 1960. _The Theory of Matrices_. Vol. I, Chelsea, New York, p. 81.

Gottlieb, D., Hussaini, M. Y. and Orszag, S. A. 1983. Theory and applications of spectral methods. Institute for Computer Applications in Science and Engineering, ICASE Report No. 83-66.

Gottlieb, D. and Orszag, S. A. 1977. Numerical analysis of spectral methods: Theory and Applications, CBMS-NSF Regional Conference Series in Applied Mathematics, SIAM, Philadelphia.

Graham, J. A. H. and Newman, B. G. 1974. Turbulent trailing vortex with central jet and wake. The Ninth Congress of the International Council of the Aeronautical Sciences, ICAS No. 74-40.

Gregory, R. T. and Karney, D. L. 1969. _A collection of matrices for testing computational algorithms_. John Wiley and Sons, p. 116.

Hama, F. R. 1962. Progressive deformation of a curved vortex filament by its own induction. _Phys. Fluids_, 5, 1156-1162.

Howard, L. N. and Gupta, A. S. 1962. On the hydrodynamic and hydromagnetic stability of swirling flows. _J. Fluid Mech_. 14, 463-476.

Hussaini, M. Y., Streett, C. L. and Zang, T. A. 1984. Spectral methods for partial differential equations. Transactions of the First Army Conference on Applied Mathematics and Computing, ARO Report 84-1.

Lamb, H. 1945. Hydrodynamics. Dover, New York, p. 592.

Lancaster, P. 1966. Lamba-matrices and vibrating systems. Pergamon Press, Oxford.

Lessen, M. and Paillet, F. 1974. The stability of a trailing line vortex. Part 2. Viscous Theory. J. Fluid Mech. 65, 769-779.

Lessen, M., Singh, P. J. and Paillet, F. 1974. The stability of a trailing line vortex. Part 1. Inviscid Theory. J. Fluid Mech. 63, 753-763.

Leuchter, O. and Solignac, J. L. 1983. Experimental investigation of the turbulent structure of vortex wakes. ONERA, TP, No. 1983-107.

Long, R. R. 1958. Vortex motion in a viscous fluid. J. Meteorology 15, 108-112.

Malik, M. R. and Poll, D. I. A. 1985. Effect of curvature on three-dimensional boundary-layer stability. AIAA Journal, 23, No. 9, 1362-1369.

Maslowe, S. A. 1974. Instability of rigidly rotating flows to non-axisymmetric disturbances. J. Fluid Mech. 64, 307-317.

Metcalfe, R. W. and Orszag, S. A. 1973. Numerical calculation of the linear stability of pipe flows. Flow Research Report No. 25.

Orszag, S. A. 1971. Accurate solution of the Orr-Sommerfeld stability equation. J. Fluid Mech. 50, 689-703.

Pedley, T. J. 1968. On the instability of rapidly rotating shear flows to non-axisymmetric disturbances. J. Fluid Mech. 31, 603-607.

Pedley, T. J. 1969. On the instability of viscous flow in a rapidly rotating pipe. J. Fluid Mech. 35, 97-115.

Rayleigh, J. W. S. 1916. On the dynamics of revolving fluids. Proc. Roy. Soc. A, 93, 148-154.

Widnall, S. E. 1972. The stability of helical vortex filament. J. Fluid Mech. 54, 641-663.

The three momentum equations plus continuity were discretized using a second order accurate central differencing. These equations are:

Continuity

$$\left(\frac{1}{2\Delta r}\right) (F_{j+1} - F_{j-1}) + \frac{1}{r_j} F_j + \frac{n}{r_j} G_j + \alpha H_j = 0 \qquad (1A)$$

r-momentum

$$\left(\frac{-i}{Re}\right) \left[\frac{F_{j+1} - 2F_j + F_{j-1}}{\Delta r^2} + \frac{F_{j+1} - F_{j-1}}{2r_j \Delta r} - \left(\frac{n^2+1}{r_j^2} + \alpha^2\right) F_j \right]$$

$$+ i \left[U_j \left(\frac{F_{j+1} - F_{j-1}}{2\Delta r}\right) + U_j' F_j \right] + \left[\omega - n \left(\frac{V_j}{r_j}\right) - \alpha W_j \right] F_j$$

$$+ 2 \left[\frac{in}{R_e r_j^2} - \left(\frac{V_j}{r_j}\right) \right] G_j + \frac{P_{j+1} - P_{j-1}}{2\Delta r} = 0, \qquad (2A)$$

θ-momentum

$$\left(\frac{-1}{Re}\right) \left[\frac{G_{j+1} - 2G_j + G_{j-1}}{\Delta r^2} + \frac{G_{j+1} - G_{j-1}}{2r_j \Delta r} - \left(\frac{n^2+1}{r_j^2} + \alpha^2\right) G_j \right]$$

$$+ U_j \left[\frac{G_{j+1} - G_{j-1}}{2\Delta r} \right] + \left[- i\omega + in \left(\frac{V_j}{r_j}\right) + i\alpha W_j + \frac{U_j}{r_j} \right] G_j$$

$$+ \left[i\, V_j' + \frac{2n}{Re\, r_j^2} \right] F_j + i\left(\frac{V_j}{r_j}\right) F_j + \left(\frac{in}{r_j}\right) P_j = 0, \tag{3A}$$

z-momentum

$$\left(\frac{-1}{Re}\right) \left[\frac{H_{j+1} - 2H_j + H_{j-1}}{\Delta r^2} + \frac{H_{j+1} - H_{j-1}}{2r_j\, \Delta r} - \left(\frac{n^2}{r_j^2} + \alpha^2\right) H_j \right]$$

$$+ U_j \left(\frac{H_{j+1} - H_{j-1}}{2\Delta r}\right) + \left[- i\omega + in\left(\frac{V_j}{r_j}\right) + \left(\frac{\partial W}{\partial r}\right)_j + i\alpha\, W_j \right] H_j$$

$$+ \left[i\left(\frac{\partial W}{\partial r}\right)_j \right] F_j + i\alpha P_j = 0. \tag{4A}$$

The resulting matrices (or system of equations) are 4N x 4N, where N is the number of grid points involved. It is obvious that even for moderate values of N the memory requirement becomes very large.

Once the code was operational, we found difficulty in obtaining a converged solution. Results of a sample calculation are given in Table 5. These results show that despite an initial decrease in the residual, it grows very fast and diverges quite rapidly. At first it was believed that the small number of grid points might have caused the problem but a substantial increase in the number of grid points showed that this was not the case. Next, attention was given to the accuracy of the method as a possible cause of the divergence. It was realized that the number of unknown factors involved (such as the number of grids, second order accuracy, boundary conditions, etc.) were too many to allow any direct checking of each factor

Table A1. Sample calculation showing convergence problem (M is the number of iterations.)

M	Residual
1	51.03473794034
2	15.83350551921
3	11.31391553601
4	8.397664066553
5	5.701436944138
6	4.314902731136
7	2.065426550367
8	1.209095939138
9	.8214686963228
10	.7912886143684
11	.6251527839796
12	.5471210004286
13	.3662554796695
14	.2757823153175
15	.1838733412282
16	.1157389438433
17	.06495193935236
18	.05683261464769
19	.0617858871914
20	.1043274836963
21	.3839152251866
22	.5645749241422
23	1.967396398417
24	6.97557243855
25	10.17577382309
26	21.72966773107
27	59.67271919984
28	151.0126448191
29	437.9075245724
30	924.9573854378
31	1850.30198365
32	4107.963293855
33	12777.07307647
34	40884.39728102
35	71145.88056394
36	119477.8852432

separately. Nevertheless, we knew that it was essential to pinpoint the exact cause of the difficulty. Therefore, a model problem was chosen so that a quick analysis of some of the above unknowns was possible in a short time; and at the same time the problem had been solved by other workers so that comparison could be made.

The temporal stability of Poiseuille flow in annulus was thought to be an ideal case for the above purpose.

APPENDIX B

AXIAL VELOCITY PROFILE IN CONCENTRIC CYLINDERS

The axial velocity for the Poiseuille flow in an annulus is given by

$$W^* = \frac{(P_1 - P_2)}{4\mu L} \left[a^2 - r^{*2} + \frac{(b^2 - a^2)}{\ln(b/a)} \ln \frac{r^*}{a} \right] \tag{1B}$$

where P_1, P_2 are the pressure, L is the length of the pipe, μ is the dynamic viscosity, a and b are the inner and outer radius, respectively and r^* is the dimensional radial distance.

Define a new variable such that

$$\xi = \frac{r^*}{a} = \frac{r(K-1)}{2} \tag{2B}$$

where

$$K = \frac{b}{a}$$

and

$$r^* = \frac{r(b-a)}{2} . \tag{3B}$$

Therefore

$$r = \frac{2r^*}{(b-a)} \tag{4B}$$

then the velocity profile is transformed to

$$W^* = \frac{(P_1 - P_2)a^2}{4\mu L} \left[1 - \xi^2 + \frac{K^2-1}{\ln(K)} \ln \xi \right] \tag{5B}$$

or

$$W = \frac{W^*}{W_0} = \left[1 - \xi^2 + \frac{K^2 - 1}{\ln(K)} \ln \xi \right].$$

41

Furthermore, it would be advantageous if we normalized the above profile with respect to the maximum velocity occurring in the annulus. Therefore

$$\frac{dW}{d\xi} = -2\xi + \frac{K^2-1}{\ell n\ K}\ \frac{1}{\xi} \tag{6B}$$

the maximum velocity occurs where

$$\frac{dW}{d\xi} = 0 = -2\xi_M + \frac{K^2-1}{\ell n\ K}\ \frac{1}{\xi_M}$$

with

$$\xi^2_M = \frac{K^2-1}{\ell n\ K^2}. \tag{7B}$$

Then evaluating the velocity

$$W_M(\xi_M) = 1 - \xi^2_M + \frac{K^2-1}{\ell n\ K}\ \ell n\ \xi_M$$

or

$$W_M(\xi_M) = 1 - \xi^2_M + \frac{K^2-1}{\ell n\ K}\ \frac{1}{2}\ \ell n\ \xi^2_M \tag{8B}$$

which results in

$$W_M(\xi_M) = 1 - \xi^2_M + \frac{K^2-1}{\ell n\ K^2}\ \ell n\ \xi^2_M.$$

With more simplification we deduce

$$W_M = 1 - \xi^2_M + \xi^2_M\ \ell n\ \xi^2_M. \tag{9B}$$

42

Now normalizing the velocity with the above maximum value, we get

$$\frac{W}{W_M} = W(\xi) = \frac{1 - \xi^2 + \xi_M^2 \, \ell n \, \xi^2}{1 - \xi_M^2 + \xi_M^2 \, \ell n \, \xi_M^2} \, . \tag{10B}$$

Since we want the non-dimensionalization to be with respect to half of the gap distance, that is

$$\frac{2a}{(b-a)} < r < \frac{2b}{(b-a)} \, . \tag{11B}$$

Then form (2B) we obtain the limits on ξ as

$$1 < \xi < K. \tag{12B}$$